Editors' Suggestion   Featured in Physics

Kerr Enhanced Backaction Cooling in Magnetomechanics

D. Zoepfl,[1,2,*] M. L. Juan,[3] N. Diaz-Naufal,[4] C. M. F. Schneider,[1,2] L. F. Deeg,[1,2] A. Sharafiev,[1,2]
A. Metelmann,[4,5,6] and G. Kirchmair[1,2,†]

[1]*Institute for Quantum Optics and Quantum Information, Austrian Academy of Sciences, 6020 Innsbruck, Austria*
[2]*Institute for Experimental Physics, University of Innsbruck, 6020 Innsbruck, Austria*
[3]*Institut Quantique and Département de Physique, Université de Sherbrooke, Sherbrooke, Québec, J1K 2R1, Canada*
[4]*Dahlem Center for Complex Quantum Systems and Fachbereich Physik, Freie Universität Berlin, 14195 Berlin, Germany*
[5]*Institute for Theory of Condensed Matter, Karlsruhe Institute of Technology, 76131 Karlsruhe, Germany*
[6]*Institute for Quantum Materials and Technology, Karlsruhe Institute of Technology, 76344 Eggenstein-Leopoldshafen, Germany*

Optomechanics is a prime example of light matter interaction, where photons directly couple to phonons, allowing the precise control and measurement of the state of a mechanical object. This makes it a very appealing platform for testing fundamental physics or for sensing applications. Usually, such mechanical oscillators are in highly excited thermal states and require cooling to the mechanical ground state for quantum applications, which is often accomplished by using optomechanical backaction. However, while massive mechanical oscillators are desirable for many tasks, their frequency usually decreases below the cavity linewidth, significantly limiting the methods that can be used to efficiently cool. Here, we demonstrate a novel approach relying on an intrinsically nonlinear cavity to backaction-cool a low frequency mechanical oscillator. We experimentally demonstrate outperforming an identical, but linear, system by more than 1 order of magnitude. Furthermore, our theory predicts that with this approach we can also surpass the standard cooling limit of a linear system. By exploiting a nonlinear cavity, our approach enables efficient cooling of a wider range of optomechanical systems, opening new opportunities for fundamental tests and sensing.

DOI: 10.1103/PhysRevLett.130.033601

Cooling mechanical modes in, or close to, their motional ground state is central for quantum applications. Even at cryogenic temperatures most systems are highly populated and further cooling is necessary. Such cooling can be achieved with feedback cooling [1–4], or using a cavity to perform sideband cooling [5,6], which works best in the so-called good cavity regime, where the mechanical frequency exceeds the cavity decay rate ($\omega_m \gg \kappa$). There, a linear cavity is desirable to allow for high photon numbers, and cooling to the ground state was shown several years ago [7,8]. As mechanical systems increase in size, their frequency naturally decreases, which inevitably brings them into the bad cavity regime ($\omega_m \ll \kappa$). There, the same cooling mechanism still applies; it is, however, limited to a finite phonon occupation due to unwanted backaction [9]. Different schemes to overcome this limitation have already been proposed, which include using two mechanical modes [10], two cavity modes [11,12], frequency modulated light [13], or entirely different coupling mechanisms such as either coupling to the cavity decay rate [14] instead of the usual dispersive coupling or coupling the mechanical system additionally to two level systems [15]. Another approach that has gained much attention is to use squeezed light created outside or even inside the cavity to improve the cooling performance [16–21].

Here, we present a fundamentally different, yet very simple, approach by using an intrinsically nonlinear cavity dispersively coupled with a mechanical system [Fig. 1(a)], proposed in [22,23]. We show that the optomechanical cooling is much more efficient than an otherwise identical linear system. Interestingly, the benefits of this nonlinear cooling scheme arise in the bad cavity regime, in contrast with another recent experiment using a nonlinear system in the good cavity regime to demonstrate cooling using four-wave mixing [24].

A nonlinear cavity dispersively coupled to a mechanical resonator [Fig. 1(a)] can be described by [23,25]

$$\hat{H}/\hbar = \omega_c \hat{a}^\dagger \hat{a} + \omega_m \hat{b}^\dagger \hat{b} + \frac{\mathcal{K}}{2}\hat{a}^\dagger \hat{a}^\dagger \hat{a}\, \hat{a} + g_0 \hat{a}^\dagger \hat{a}(\hat{b}^\dagger + \hat{b}) + \hat{H}_d.$$

$$(1)$$

Here, $\hat{a}^\dagger(\hat{a})$ and $\hat{b}^\dagger(\hat{b})$ are the creation (annihilation) operators of the cavity and the mechanical resonator and the respective frequencies are given by ω_c and ω_m. The nonlinearity of the cavity is introduced by the Kerr constant $\mathcal{K}$, leading to a frequency shift per photon. The coupling strength between the two systems is given by the single-photon coupling strength g_0 and $\hat{H}_d$ is an external drive.
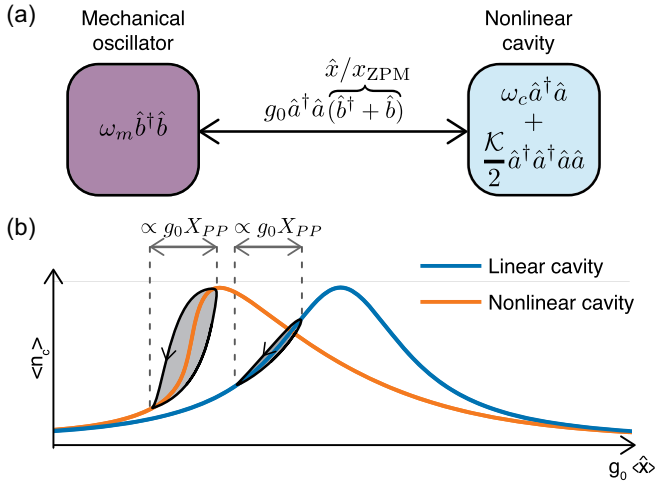
FIG. 1. Nonlinear cooling illustration. (a) Optomechanical interaction between a mechanical oscillator and a nonlinear cavity. (b) To illustrate the enhanced cooling, we compare the response of the cavity photon number, n_c, of a linear to an identical nonlinear cavity. The cavity frequency changes due to the optomechanical interaction ($g_0 \langle \hat{x} \rangle$), changing the probe-cavity detuning. For the linear case we recover a symmetric response, while for the nonlinear one the typical nonlinear response. This is identical to sweeping the probe tone itself through a fixed frequency cavity. The shaded area indicates the cooling work done on a mechanical system within a cycle by the cavity for parameters from the experiment. X_{PP} denotes the peak-to-peak amplitude of the mechanical resonator. The cooling enhancement provided by the nonlinearity is clearly visible.

The position operator of the mechanical mode translates as $\hat{x} = x_{\mathrm{zpm}}(\hat{b}^\dagger + \hat{b})$, where x_{zpm} is the mechanical zero point motion. Additional information is given in the Supplemental Material [26].

For an intuitive picture of the nonlinear cooling we consider the cavity response to a fixed frequency probe tone, while the optomechanical interaction changes the probe-cavity detuning [Fig. 1(b)]. In case of a completely linear system, a symmetric response is recovered, identical to the response when sweeping a probe tone over a fixed frequency cavity. The origin of the cooling can be understood as a time lag of the cavity photons due to a finite cavity lifetime [27]. The shaded area depicts the cooling work done on the mechanical system within one cycle for an ideal red detuned probe tone, which we simulate with a simple model [26] using parameters closely related to the experiment. Now, let us consider a cavity with a negative Kerr, such that the cavity is close to bistability [28] (i.e., where the response of the cavity gets infinitely steep at a certain detuning) using otherwise the same parameters as for the linear case discussed previously. Probing this system with a fixed frequency tone, we obtain the typical nonlinear response. For lower drive strengths the cavity would be effectively linear, while for higher drives bistability is reached and two metastable states appear in a certain range

of detunings. As the enclosed area within one cycle increases, it is evident that the cooling is enhanced compared to the linear case. Because of the nonlinear line shape, small changes of the cavity frequency related to the mechanical motion induce a large variation of the cavity photon number, which not only increases the cooling itself, but also suppresses the unwanted backaction heating. Working on the blue side (i.e., frequency of the probe tone above the cavity frequency), the cavity slope is effectively more shallow compared to the linear case, leading to a decrease of the heating backaction. Alternatively, the nonlinear enhanced cooling can also be explained via the usual scattering picture. Because of the nonlinearity, the density of states of the cavity is asymmetric, which impacts the Stokes and anti-Stokes rates. Additionally, due to the mechanical oscillation, the photon number changes, which is given by the very asymmetric shape of the intracavity photon number. The combination of both effects leads to the enhancement of the cooling performance, using a nonlinear cavity [25]. For a positive Kerr, this effect would be entirely reversed.

The setup consists of a superconducting microstrip cavity coupled to a single clamped beam—a cantilever— with a magnet on its tip [Figs. 2(a) and 2(b)], similar to the setup discussed in [29,40]. A superconducting quantum interference device (SQUID) embedded in the cavity makes it sensitive to magnetic fields, mediating the inductive coupling to the cantilever. Recently also other experimental realizations using inductively coupled optomechanical systems have been demonstrated [24,41,42]. Our setup is mounted to the base plate of a dilution refrigerator, kept at 100 mK for most of the experiments, where the system is very stable and the mechanical mode is well thermalized. The cavity has a frequency of $\omega_c/2\pi = 8.176$ GHz with a linewidth of $\kappa/2\pi = 3.5$ MHz, while the cantilever has a frequency of $\omega_m/2\pi = 274.41$ kHz with a linewidth of approximately $\Gamma_m/2\pi = 0.4$ Hz, which means that the setup resides deep in the bad cavity regime. In Fig. 2(c) we show the dependence of the cavity frequency on the magnetic field, which also tunes its sensitivity and determines, up to a prefactor, the coupling rate. So far we directly measured single-photon coupling strengths of up to 7.4 kHz, while the sensitivity of the cavity allows couplings exceeding 90 kHz [26]. Excessive flux noise does not allow for a stable operation at those flux sensitivities, where we estimate a flux noise of $302 \pm 19 \, \mu\phi_0$, which is mainly induced by mechanical vibrations [26].

Another aspect of a SQUID is its nonlinearity with regard to input power, since its inductance also depends on the number of photons circulating in the cavity. As the number of photons in the cavity increases, the frequency shifts to lower values, leading to the nonlinear response when scanning a sufficiently strong probe tone across [Fig. 2(d)]. This effect leads to an enhanced cooling, as discussed previously (Fig. 1).
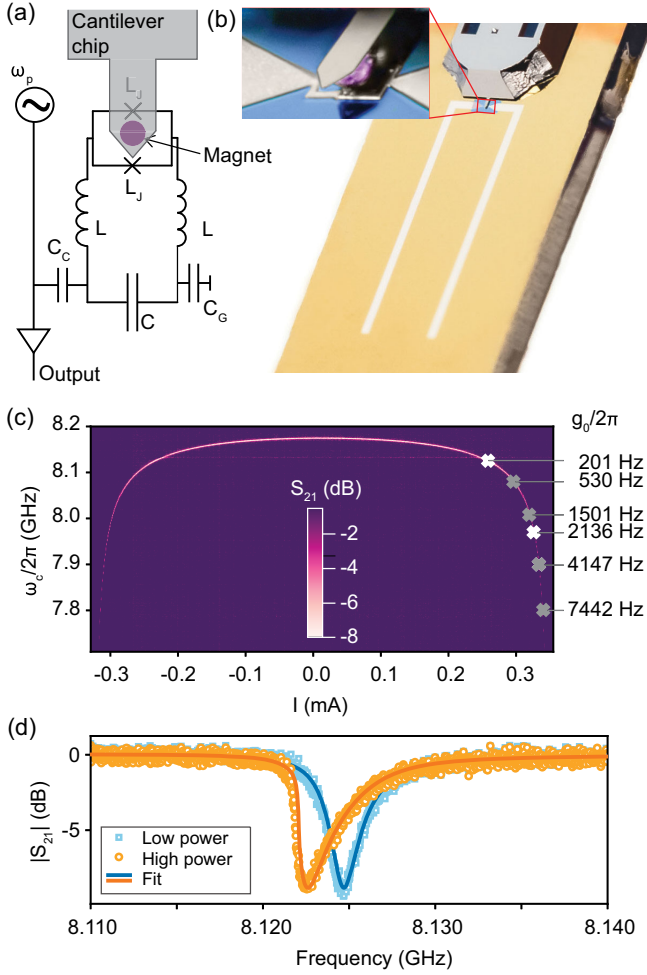
FIG. 2. Setup and characterization. (a) Schematic depiction of our setup. L and L_J are the cavity and the junction inductance, C, C_c, and C_G denote the self capacitance of the cavity, the coupling, and the ground capacitance. (b) Picture of the microstrip cavity (white) on top of a silicon substrate (golden). The cantilever chip (gray) is glued to the silicon substrate. An optical microscope picture (enlargement) shows the cantilever with false colored magnet above the SQUID loop. (c) Change of cavity frequency when applying external magnetic flux. Indicated are the measured coupling values g_0 as the flux sensitivity changes. White crosses symbolize measurements presented in the main text, gray crosses in [26]. (d) Characterization of the cavity nonlinearity. Close to bistability, the response is in good agreement with the model for a Kerr nonlinear cavity [26]. For low drive powers we effectively recover a linear response.

We measure the cantilever motion by taking a homodyne noise spectrum of the probe tone, where the mechanical signature appears as an amplitude (phase) modulation sideband [29] and fit this sideband with the model of a damped harmonic oscillator [30]. To investigate the back-action, we measure the mechanical cantilever for different detunings between the probe tone and the cavity. Taking such cooling traces for several powers up to bistability reveals the cooling enhancement due to the nonlinearity.
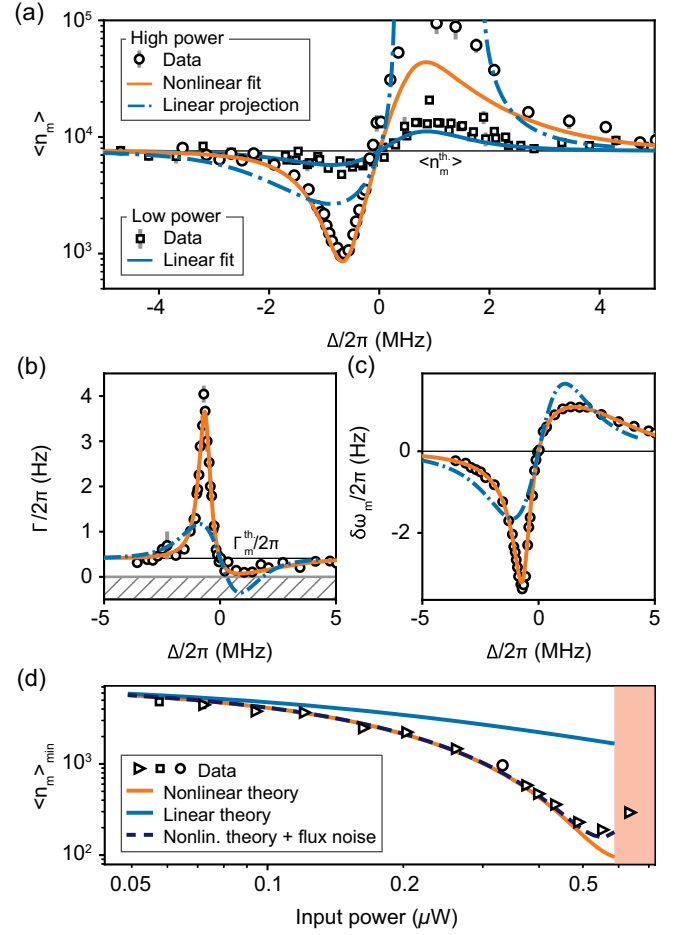

FIG. 3. Nonlinear cooling measurement at $g_0/2\pi = 201 \pm 3$ Hz. (a) Phonon number $\langle n_m \rangle$ against probe-cavity detuning, Δ, for two powers. (b),(c) Mechanical linewidth and frequency against probe-cavity detuning for the high power case. The suppressed heating prevents us from entering the instable regime ($\Gamma/2\pi < 0$). (d) Lowest phonon number, $\langle n_m \rangle_{\min}$, for different input power. Right before bistability (shaded region), the cooling is limited by flux noise, which is captured in a simple model [26]. The errors shown are the standard errors [26].

For this measurement, we work at a moderate coupling of 201 ± 3 Hz to avoid limiting effects from flux noise, where the cavity shows a Kerr nonlinearity of $\mathcal{K}/2\pi = -12.2 + 0.1$ kHz/photon. Figure 3(a) shows such cooling traces for two different powers. For the low power measurement, the cavity is effectively in the linear regime and thus the cooling curve agrees well with linear theory [5,43]. Conversely, in the high power regime only the nonlinear theory describes the measurement data accurately. Assuming a linear cavity but otherwise identical parameters would predict much weaker cooling and much stronger heating than what we observe. We note that in this regime the cooling happens over a much narrower range of detunings such that a fit with the linear theory is not in good agreement with the data [26]. In Figs. 3(b) and 3(c) we plot the change of mechanical linewidth and frequency for the

high power measurement. Again, we only observe good agreement with the nonlinear theory. We further clearly demonstrate the asymmetry in backaction strength when either working red detuned (cooling) or blue detuned (heating) with respect to the cavity as expected for a negative Kerr, already illustrated in Fig. 1.

In Fig. 3(d) we show the lowest phonon number measured for each cooling trace [26] against the input power together with the predictions from the linear and nonlinear theory. For increasing power, we clearly see the cooling enhancement due to the nonlinear cavity, reaching strongest cooling just before bistability. There, we outperform a conventional linear system by more than an order of magnitude, making the nonlinear cooling a very efficient cooling scheme. To properly model the impact of flux noise at high input power, we include a Gaussian distribution for the detuning instead of a fixed value, which reproduces the measurement data well [26].

To explore the limits of the system, we move to higher couplings, where we expect an increased backaction and thus increased cooling, but at the cost of higher sensitivity to flux noise. To reach the lowest phonon occupation currently possible in our setup, we use a coupling of $g_0/2\pi = 2136 \pm 26$ Hz and decrease the temperature of our cryostat to 40 mK. This is doubly beneficial since the thermal phonon occupation and the linewidth of the cantilever become smaller, reducing the impact of the environment [26]. What further helps us is a slight anomaly in the Kerr. In this region we still have the discussed benefits of a nonlinear system but with a smaller Kerr, which allows us to drive the system even harder, together with a high coupling strength. The disadvantage here is that the anomalous Kerr prevents us from modeling the full system as in Fig. 3 [26].

In Fig. 4(a) we show three mechanical noise spectral densities with increasing cooling backaction by increasing the input power and changing the probe-cavity detuning, starting with a thermal spectral density. In Fig. 4(b) we plot a spectral density for one of the lowest phonon occupation numbers we can currently reach, which is heavily influenced by flux noise. Thus, instead of the usual fit, we extract the phonon number in two different ways: by directly integrating the area below the peak and by fitting the data using a model including flux noise [26]. Both methods show good agreement and give an occupation of around 14 phonons, around 200 times below the thermal occupation.

Finally, we theoretically investigate the full capabilities of nonlinear cooling without the limiting factors of flux noise and hence also the possibilities of increasing g_0 further. In Fig. 4(c) we show the lowest phonon number achievable for increasing coupling. For the nonlinear theory, shown in orange, we vary the power (dotted line) to minimize the phonon number while operating to at most 99% of the bistable power. For comparison, the linear cooling using the same power is shown in blue, providing at low g_0 a less efficient cooling, something that was already
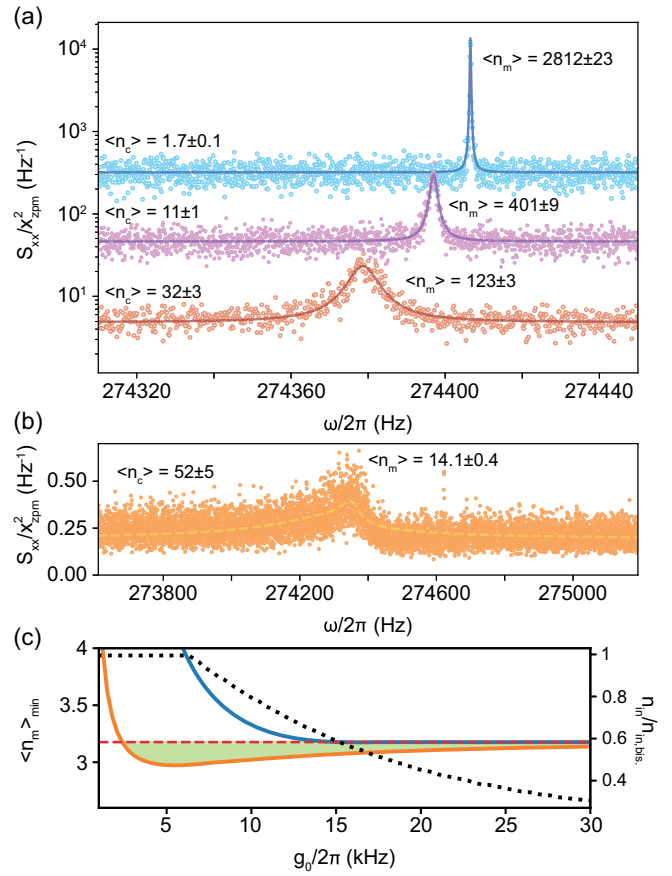

FIG. 4. Best cooling using higher g_0. (a) Mechanical noise spectral densities and corresponding fits at 40 mK and $g_0/2\pi = 2136 \pm 26$ Hz for increasing backaction by changing the input power and the probe-cavity detuning. The noise floor decreases with increasing backaction, which is also a result of our cavity acting as a parametric amplifier [44]. $\langle n_c \rangle$ are the average number of photons circulating in the cavity for the measurement; the uncertainties arise from uncertainties in the input photon number, linewidth, and detuning. The uncertainties for the phonon numbers are fit errors. (b) Spectral density for one of the lowest mechanical occupation numbers we measured. We fit this trace with a model including flux noise (dashed, [26]). The uncertainty on the phonon number comes from the uncertainty of the offset determination for the numeric integration [26]). (c) Theory prediction for the lowest phonon occupation reachable when increasing g_0 always using the optimal input power for the nonlinear case ($\mathcal{K}/2\pi = -12$ kHz/n_c) up to bistability (orange, the dotted line is the input power). For the comparison to linear theory we either use the same power (blue line) or the ideal power for the linear case (red dashed). All other parameters remain constant. Nonlinear cooling allows cooling to $\langle n_m \rangle = 2.97$, while in the linear case cooling is limited to 3.18 phonons.

observed in the experimental data (Fig. 3). Remarkably, when not limiting the power used for the linear cavity to minimize the phonon occupation (red dashed line), the nonlinear cavity still provides better cooling. Thus, nonlinear cooling is not only more efficient, but also allows one to reach a lower phonon number in the bad cavity limit.

To conclude, we demonstrate a novel way of cooling an optomechanical system by using an intrinsically nonlinear cavity. We show that the nonlinearity has to be crucially taken into account when describing optomechanical back-action on the mechanical cantilever and demonstrate a tenfold cooling enhancement compared to an otherwise identical linear system. By increasing the coupling, we show cooling of the mechanical occupation from 2800 thermal phonons to 14 phonons. However, not only does flux noise prevent us from cooling to lower occupation, it also restricts us from operating at even higher couplings, while the sensitivity of our cavity allows for a single-photon coupling strength exceeding 90 kHz. There, we would reach single-photon quantum cooperativity exceeding unity when working at 40 mK and assuming that we reduce our flux noise by a factor of 2.

Interestingly, for some region of coupling strengths, the nonlinear cooling even beats the standard cooling limit of a linear system by a small amount, where the region can be tuned by the nonlinearity. This combines an optomechanical system in the bad cavity regime with a nonlinear cavity, which are separately often considered as unfavorable. Furthermore, previous work [21] has experimentally demonstrated that externally generated squeezed light injected into the cavity can eliminate unwanted backaction. In this context, it will be interesting to study whether or not internal squeezing that can be generated in Kerr cavities can be applied as a resource for enhanced cooling. This approach is especially relevant when working with massive mechanical systems, which are essential for many tests of fundamental physics and sensing applications [31,45–49].

*Corresponding author.
david.zoepfl@uibk.ac.at
†Corresponding author.
gerhard.kirchmair@uibk.ac.at

[1] S. Mancini, D. Vitali, and P. Tombesi, Optomechanical Cooling of a Macroscopic Oscillator by Homodyne Feedback, Phys. Rev. Lett. **80**, 688 (1998).

[2] P. F. Cohadon, A. Heidmann, and M. Pinard, Cooling of a Mirror by Radiation Pressure, Phys. Rev. Lett. **83**, 3174 (1999).

[3] F. Tebbenjohanns, M. Frimmer, V. Jain, D. Windey, and L. Novotny, Motional Sideband Asymmetry of a Nanoparticle Optically Levitated in Free Space, Phys. Rev. Lett. **124**, 013603 (2020).

[4] M. Rossi, D. Mason, J. Chen, Y. Tsaturyan, and A. Schliesser, Measurement-based quantum control of mechanical motion, Nature (London) **563**, 53 (2018).

[5] F. Marquardt, J. P. Chen, A. A. Clerk, and S. M. Girvin, Quantum Theory of Cavity-Assisted Sideband Cooling of Mechanical Motion, Phys. Rev. Lett. **99**, 093902 (2007).

[6] I. Wilson-Rae, N. Nooshi, W. Zwerger, and T. J. Kippenberg, Theory of Ground State Cooling of a Mechanical Oscillator Using Dynamical Backaction, Phys. Rev. Lett. **99**, 093901 (2007).

[7] J. D. Teufel, T. Donner, D. Li, J. W. Harlow, M. S. Allman, K. Cicak, A. J. Sirois, J. D. Whittaker, K. W. Lehnert, and R. W. Simmonds, Sideband cooling of micromechanical motion to the quantum ground state, Nature (London) **475**, 359 (2011).

[8] J. Chan, T. P. M. Alegre, A. H. Safavi-Naeini, J. T. Hill, A. Krause, S. Gröblacher, M. Aspelmeyer, and O. Painter, Laser cooling of a nanomechanical oscillator into its quantum ground state, Nature (London) **478**, 89 (2011).

[9] M. Aspelmeyer, T. J. Kippenberg, and F. Marquardt, Cavity optomechanics, Rev. Mod. Phys. **86**, 1391 (2014).

[10] T. Ojanen and K. Børkje, Ground-state cooling of mechanical motion in the unresolved sideband regime by use of optomechanically induced transparency, Phys. Rev. A **90**, 013824 (2014).

[11] J.-Y. Yang, D.-Y. Wang, C.-H. Bai, S.-Y. Guan, X.-Y. Gao, A.-D. Zhu, and H.-F. Wang, Ground-state cooling of mechanical oscillator via quadratic optomechanical coupling with two coupled optical cavities, Opt. Exp. **27**, 22855 (2019).

[12] Y.-C. Liu, Y.-F. Xiao, X. Luan, Q. Gong, and C. W. Wong, Coupled cavities for motional ground-state cooling and strong optomechanical coupling, Phys. Rev. A **91**, 033818 (2015).

[13] D.-Y. Wang, C.-H. Bai, S. Liu, S. Zhang, and H.-F. Wang, Optomechanical cooling beyond the quantum backaction limit with frequency modulation, Phys. Rev. A **98**, 023816 (2018).

[14] F. Elste, S. M. Girvin, and A. A. Clerk, Quantum Noise Interference and Backaction Cooling in Cavity Nanomechanics, Phys. Rev. Lett. **102**, 207209 (2009).

[15] C. Genes, H. Ritsch, and D. Vitali, Micromechanical oscillator ground-state cooling via resonant intracavity optical gain or absorption, Phys. Rev. A **80**, 061803 (2009).

[16] B. Xiong, X. Li, S.-L. Chao, Z. Yang, R. Peng, and L. Zhou, Strong squeezing of duffing oscillator in a highly dissipative optomechanical cavity system, Ann. Phys. (Berlin) **532**, 1900596 (2020).

[17] M. Asjad, N. E. Abari, S. Zippilli, and D. Vitali, Optomechanical cooling with intracavity squeezed light, Opt. Exp. **27**, 32427 (2019).

[18] M. Asjad, S. Zippilli, and D. Vitali, Suppression of Stokes scattering and improved optomechanical cooling with squeezed light, Phys. Rev. A **94**, 051801 (2016).

[19] S. Huang and G. S. Agarwal, Enhancement of cavity cooling of a micromechanical mirror using parametric interactions, Phys. Rev. A **79,** 013821 (2009).

[20] J.-H. Gan, Y.-C. Liu, C. Lu, X. Wang, M. K. Tey, and L. You, Intracavity-Squeezed Optomechanical Cooling, Laser Photonics Rev. **13,** 1900120 (2019).

[21] J. B. Clark, F. Lecocq, R. W. Simmonds, J. Aumentado, and J. D. Teufel, Sideband cooling beyond the quantum backaction limit with squeezed light, Nature (London) **541,** 191 (2017).

[22] C. Laflamme and A. A. Clerk, Quantum-limited amplification with a nonlinear cavity detector, Phys. Rev. A **83,** 033803 (2011).

[23] P. D. Nation, M. P. Blencowe, and E. Buks, Quantum analysis of a nonlinear microwave cavity-embedded dc SQUID displacement detector, Phys. Rev. B **78,** 104516 (2008).

[24] D. Bothner, I. C. Rodrigues, and G. A. Steele, Four-wave-cooling to the single phonon level in Kerr optomechanics, Commun. Phys. **5,** 33 (2022).

[25] N. Diaz-Naufal, D. Zoepfl, M. L. Juan, C. M. F. Schneider, L. F. Deeg, G. Kirchmair, and A. Metelmann (to be published).

[26] See Supplemental Material at http://link.aps.org/supplemental/10.1103/PhysRevLett.130.033601, which includes Refs. [5,22–25,28–30,32–40,43], for additional information on the setup, the nonlinear cooling theory, the data analysis, the flux noise model, and supplementary measurement data.

[27] F. Marquardt, A. Clerk, and S. Girvin, Quantum theory of optomechanical cooling, J. Mod. Opt. **55,** 3329 (2008).

[28] P. R. Muppalla, O. Gargiulo, S. I. Mirzaei, B. P. Venkatesh, M. L. Juan, L. Grünhaupt, I. M. Pop, and G. Kirchmair, Bistability in a mesoscopic Josephson junction array resonator, Phys. Rev. B **97,** 024518 (2018).

[29] D. Zoepfl, M. L. Juan, C. M. F. Schneider, and G. Kirchmair, Single-Photon Cooling in Microwave Magnetomechanics, Phys. Rev. Lett. **125,** 023601 (2020).

[30] M. L. Gorodetsky, A. Schliesser, G. Anetsberger, S. Deleglise, and T. J. Kippenberg, Determination of the vacuum optomechanical coupling rate using frequency noise calibration, Opt. Express **18,** 23236 (2010).

[31] A. G. Krause, M. Winger, T. D. Blasius, Q. Lin, and O. Painter, A high-resolution microchip optomechanical accelerometer, Nat. Photonics **6,** 768 (2012).

[32] S. Probst, F. B. Song, P. A. Bushev, A. V. Ustinov, and M. Weides, Efficient and robust analysis of complex scattering data under noise in microwave resonators, Rev. Sci. Instrum. **86,** 024706 (2015).

[33] C. W. Gardiner, Driving a Quantum System with the Output Field from Another Driven Quantum System, Phys. Rev. Lett. **70,** 2269 (1993).

[34] https://scipy.org/.

[35] C. W. Gardiner and M. J. Collett, Input and output in damped quantum systems: Quantum stochastic differential equations and the master equation, Phys. Rev. A **31,** 3761 (1985).

[36] https://scikit-learn.org/.

[37] *Model Selection and Multimodel Inference,* edited by K. P. Burnham and D. R. Anderson (Springer, New York, NY, 2004).

[38] V. Kornev and A. Arzumanov, Numerical simulation of Josephson-junction system dynamics in the presence of thermal noise, Inst. Phys. Conf. Ser. **158,** 627 (1997).

[39] S. V. Polonsky, V. K. Semenov, and P. N. Shevchenko, PSCAN: Personal superconductor circuit analyser, Supercond. Sci. Technol. **4,** 667 (1991).

[40] D. Zoepfl, P. R. Muppalla, C. M. F. Schneider, S. Kasemann, S. Partel, and G. Kirchmair, Characterization of low loss microstrip resonators as a building block for circuit QED in a 3D waveguide, AIP Adv. **7,** 085118 (2017).

[41] T. Bera, S. Majumder, S. K. Sahu, and V. Singh, Large flux-mediated coupling in hybrid electromechanical system with a transmon qubit, Commun. Phys. **4,** 12 (2021).

[42] T. Luschmann, P. Schmidt, F. Deppe, A. Marx, A. Sanchez, R. Gross, and H. Huebl, Mechanical frequency control in inductively coupled electromechanical systems, Sci. Rep. **12,** 1608 (2022).

[43] A. H. Safavi-Naeini, J. Chan, J. T. Hill, S. Gröblacher, H. Miao, Y. Chen, M. Aspelmeyer, and O. Painter, Laser noise in cavity-optomechanical cooling and thermometry, New J. Phys. **15,** 035007 (2013).

[44] M. Hatridge, R. Vijay, D. H. Slichter, J. Clarke, and I. Siddiqi, Dispersive magnetometry with a quantum limited SQUID parametric amplifier, Phys. Rev. B **83,** 134501 (2011).

[45] M. F. Gely and G. A. Steele, Superconducting electromechanics to test Diósi–Penrose effects of general relativity in massive superpositions, AVS Quantum Sci. **3,** 035601 (2021).

[46] O. Romero-Isart, Quantum superposition of massive objects and collapse models, Phys. Rev. A **84,** 052121 (2011).

[47] I. Pikovski, M. R. Vanner, M. Aspelmeyer, M. S. Kim, and Č. Brukner, Probing Planck-scale physics with quantum optics, Nat. Phys. **8,** 393 (2012).

[48] M. Arndt and K. Hornberger, Testing the limits of quantum mechanical superpositions, Nat. Phys. **10,** 271 (2014).

[49] C. Whittle *et al.,* Approaching the motional ground state of a 10-kg object, Science **372,** 1333 (2021).